Photoluminescent studies on porous silicon/tin oxide heterostructures

V.S. Vidhya[a], K.R. Murali[b], B. Subramanian[b], P. Manisankar[a], C. Sanjeeviraja[c], M. Jayachandran[b],*

[a] School of Chemistry, Alagappa University, Karaikudi 630 003, India
[b] Electrochemical Materials Science Division, Central Electrochemical Research Institute (Council of Scientific and Industrial Research, New Delhi), Karaikudi 630 006, India
[c] School of Physics, Alagappa University, Karaikudi 630 003, India

ABSTRACT

Porous silicon (PSi) structure was formed at different current densities in the range of 5–60 mA/cm^2 by the electrochemical anodization of PSi wafers etching in HF for 30 min. The PSi was characterized by X-ray diffraction studies. The PSi samples prepared at current densities above and below 30 mA/cm^2 show PL spectra with asymmetric and overlapped peaks. On the top surface as well as inside the pores of this PSi structures the precursor sol–gel was incorporated by the spin coating technique and SnO$_2$ was formed by heating at 400 °C in air. Peaks pertaining to PSi along with those corresponding to SnO$_2$ were observed, which confirmed SnO$_2$ formation as thin film on the PSi surface. The PL spectra of SnO$_2$/PSi structure aged for two months indicated a reduction in PL intensity but remained constant afterwards. SnO$_2$ not only modifies the nature of silicon nanopores but also is expected to influence the interface states in SnO$_2$/PSi junction.

© 2010 Elsevier B.V. All rights reserved.

1. Introduction

During the last decade, there has been a rapid increase in the study of porous silicon (PSi) structures. To take benefit from the intense red photoluminescence (PL) of PSi at room temperature [1], many attempts have been made to introduce PSi in the circuitry of some silicon-based optoelectronic devices. Indium tin oxide (ITO) or semitransparent Au electrodes were frequently used as transparent conducting electrodes in PSi-based LED structures [2,3]. These electrodes can be deposited by various methods such as chemical vapor deposition, sputtering or thermal evaporation. In a previous report, the significance of the sol–gel (SG) technique for the growth of Sb-doped (SnO$_2$:Sb) or ITO into nanoporous silicon [4] was demonstrated. The formation of SnO$_2$:Sb on PSi with different porosities has been recently reported [5], in which the SnO$_2$:Sb film has been beneficial in preserving the PL and EL characteristics.

In this work, we investigate the use of the sol–gel spin coating method to obtain very thin SnO$_2$ layers in the nanometric pores of the PSi. The effect of SnO$_2$ layers on the photoluminescence properties of PSi is studied.

2. Experimental methods

Porous silicon structures were formed on the surface of p-type Si (1 0 0) wafers, with a resistivity of 0.05–0.07 Ω cm by electrochemical anodic etching process. A 1:2 mixture of 30% hydrofluoric acid and ethanol was used as the etching electrolyte.

Aluminium film was evaporated on the back side of the Si wafers to improve the uniformity of the anodic current. Galvanostatic etching was carried out for 30 min with the current densities of 5, 10, 30, 45 and 60 mA/cm^2 in the dark. The weight of the silicon before and after etching was measured using a Mettler semi micro balance. The freshly prepared PSi wafers were fixed horizontally to the turntable of the spin coater. Few drops of sol–gel precursors were dropped on the PSi surface and rotated at 3500 rpm for 10 s. The PSi structure filled with the sol–gel precursors was heated in air at 400 °C for 15 min. These SnO$_2$/PSi structures were further characterized for their PL and structural studies. The structures were characterized by X-ray diffraction (XRD) studies using CuKα radiation form an Xpert PANanalytical XRD unit. Surface morphology of the films was studied by HITACHI Model S-3000H SEM instrument. PL studies were made at room temperature using Varian Cary Eclipse Fluorescence Spectrophotometer. PL spectra were recorded using 425 nm excitation.

3. Results and discussion

PSi structures were formed on p-type silicon single crystal wafers with (1 0 0) orientation. Fig. 1b–f shows the XRD pattern for the surfaces etched at current densities of 5, 10, 30, 45 and 60 mA/cm^2, respectively. A sharp and highly intense (1 0 0) peak corresponding to silicon single crystal is observed for the unetched Si wafer (Fig. 1a). XRD patterns of the PSI structures show distinctive behaviour between the single crystal surface and the etched surface. At very low current density of 5 mA/cm^2, the etching force is very small which is sufficient enough to perturb the whole surface into fragments. This is supported by the enlarged width and reduced intensity of the (1 0 0) peak (Fig. 1b). At 10 mA/cm^2, pore formation starts and the entire surface shows sponge like structure. This is evident from the broad peak at 69.9° revealing a non-crystalline like structure at the same 'd' value, where the single crystalline peak is observed. Further, the broad peak is shifted to

* Corresponding author. Tel.: +91 4565227550.
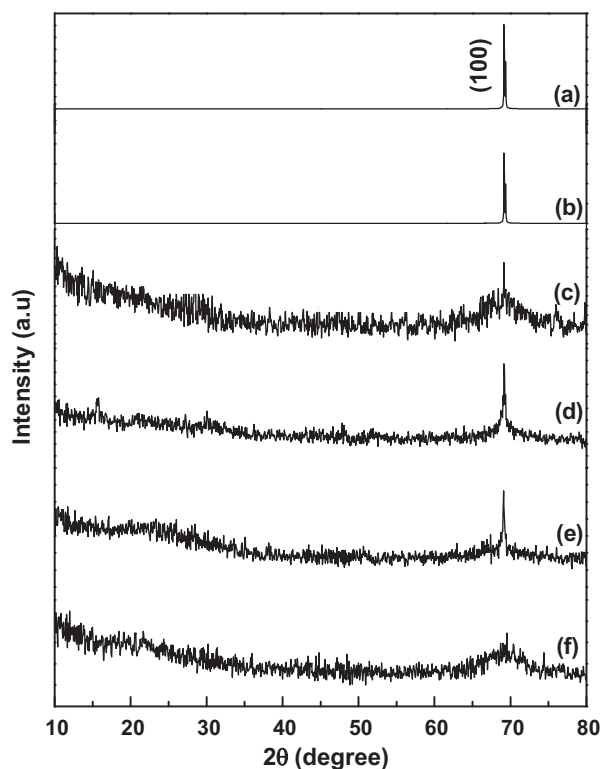 *E-mail address:* mjayam54@yahoo.com (M. Jayachandran).

Fig. 1. XRD pattern of (a) single crystal silicon and PSi structures formed at (b) 5, (c) 10, (d) 30, (e) 45, and (f) 60 mA/cm^2.

Fig. 2. XRD pattern of SnO_2/PSi structure.

pits and also between the pits which are not observed in these SEM pictures. Fig. 3a shows the initiation of etch pits all over the Si surface etched at 5 mA/cm^2. At 10 mA/cm^2, the pore formation starts (Fig. 3b) which makes uniform pores at 30 mA/cm^2 with thin silicon networks (Fig. 3c). When the current density is increased beyond this, the surface once again becomes scattered with less

lower 2θ value. This characteristic confirms that nanocrystalline silicon particles are formed inside the pores after affecting some dissolution at the surface. When the current density is increased to 45 mA/cm^2, the top layer of PSi structure is dissolved and the bottom surface near to silicon substrate is exposed. In this case the particles would be slightly larger in size. This is explicit from the increased intensity and reduced width (FWHM) of the (1 0 0) peak. At very high current densities (60 mA/cm^2), dissolution of the top porous surface takes place and the inner silicon surface with large number of pits and tiny silicon grains are exposed. This is confirmed by the appearance of the broad feature at (1 0 0) peak along with a small peak.

The presence of a peak corresponding to (1 0 0) plane and the recorded shift to lower angles, as observed in Fig. 1, confirm that the cubic structure of the starting single crystal silicon is retained in all the porous silicon structures also [6]. This observed shift is in accordance with the results of XRD rocking curves obtained by Buttard et al. [7] in which two sharp peaks pertaining to Si substrate and PSi layer are present. In the case of the SnO_2 coated PSi, it is expected that a very thin layer of SnO_2 is also formed over the PSi structure after filling the inner walls of the pores as well. To ascertain the incorporation of SnO_2 into the pores, XRD studies were conducted and the XRD pattern is shown in Fig. 2. The peaks pertaining to PSi are seen at 69.9° (1 0 0) along with the SnO_2 peak at 26.58° (1 1 0). These observations are in good agreement with the results observed for nanocrystalline SnO_2 powder [8] and pulse laser deposited (PLD) SnO_2 films on Si (1 0 0) substrates [9]. The size of the SnO_2 nanocrystallites obtained using Scherrer's equation is 10 nm.

Fig. 3a–c shows the SEM surface morphology of PSi structures formed at different current densities for 30 min. The surfaces are rather well packed structures of nearly circular pores separated by thin column of walls. The dimensions of the pores vary from 5 to 20 μm. There may be columnar structures of silicon inside the
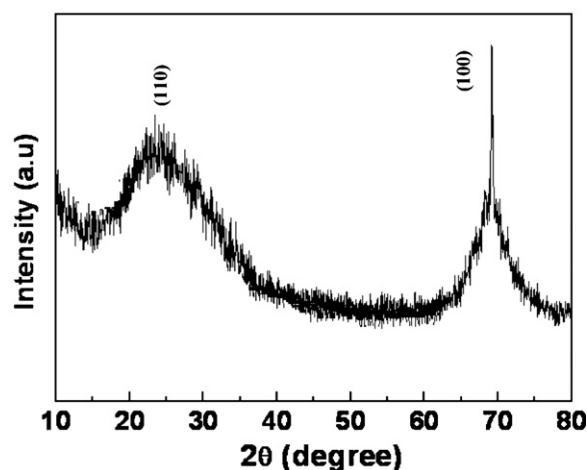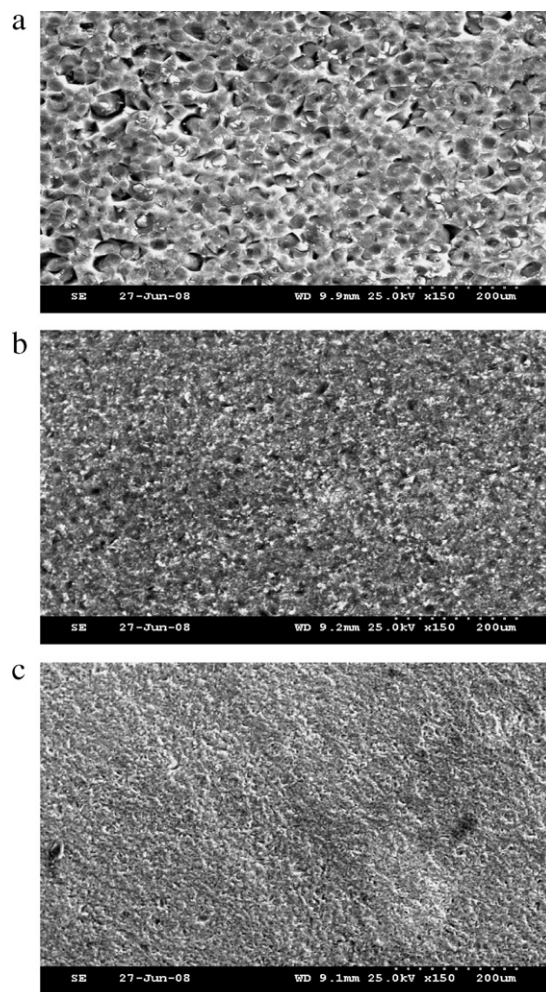

Fig. 3. SEM pictures of PSi structures formed with current densities (a) 5, (b) 10 and (c) 30 mA/cm^2.

Fig. 4. Photoluminescence spectra of PSi structures formed at (a) 5, (b) 10, (c) 30, (d) 45 and (e) 60 mA/cm^2.

Fig. 5. Photoluminescence emission spectra of PSi structures (a) freshly formed, (b) heated at 600 °C for 5 h, (c) aged for one month and (d) aged for two months (a–d, top to bottom).

pore size or with wider silicon network. This may be due to the dissolution of top silicon PSi layer at higher current densities and the bottom surface near to the silicon being exposed.

PSi structures are reported to luminescent in the near infrared (0.8 eV) and in the whole visible range called S-band [10]. The PL properties of PSi structures formed at different current densities, their aging effect and the behaviour of SnO$_2$/PSi surface are reported.

Visual observation of the PSi showed a golden brownish area for various current densities. The observed PL spectra at room temperature at all the current densities confirm the formation of PSi structures with nanocrystalline features. PL spectra were recorded using 425 nm excitation spectrum corresponding to an energy of 2.7 eV.

Fig. 4 shows the PL spectra of PSi structures formed at 5, 10, 30, 45, and 60 mA/cm^2 for 30 min. The corresponding peaks are observed at 699, 656, 630, 651 and 645 nm, respectively. It shows a bandgap tuning with etching current (1.77–1.97 eV). The intensity increases up to 30 mA/cm^2 and then decreases. The initial shift in the luminescence towards the blue region can be explained in terms of the formation of small grains at 30 mA/cm^2 compared to 5 mA/cm^2 and 10 mA/cm^2 where the pore formation had just begun. Further shift of the luminescence peak towards red region at current densities greater than 30 mA/cm^2 may be due to the dissolution of top silicon PSi layer and the bottom surface near to the silicon being exposed, containing larger grains. Similar type of variation has been observed earlier [11].

At 30 mA/cm^2, a single-peak profile (Fig. 4c) shows the formation of silicon nanocrystallites uniformly distributed over the entire surface. The PSi samples prepared at current densities above and below 30 mA/cm^2 show PL spectra with asymmetric and overlapped peaks. It means that, in such PSi surface profile, there is the presence of a set of semi-isolated silicon nanocrystallites with different dimensions or shapes [12]. Each set of such silicon crys-
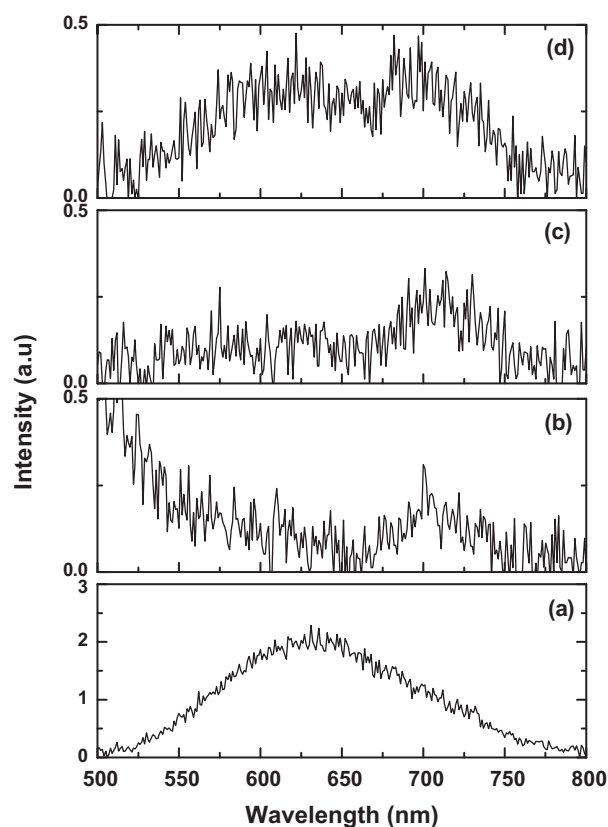
tals consists of a narrow distribution of similar dimensions and contribute to one of the PL peaks in the broad PL spectra [13–15].

Further, the size variation of the nanocrystallites was determined on the assumption that each particle constituting the PSi gives a sharp luminescence peak. Our XRD results show the particle size variation increasing with current density which is maximum for the PSi structure formed at 30 mA/cm^2 in the present study. These detailed studies of PL conclude that PSi structure formed at 30 mA/cm^2 for 30 min can produce the quality PSi substrates with maximum PL useful for solar cell fabrication.

The effect of rapid thermal treatment in air and exposure to open atmosphere for two months is studied. PL spectra of freshly prepared PSi layer, heated at 600 °C for 5 h, aged for one month and two months are shown in Fig. 5a–d, respectively. Heating reduces the PL intensity and shifts the peak to higher wavelength side from 630 to 700 nm with some humps in the lower wavelength side as well. After aging for one month and two months, pronounced PL peaks are observed on both sides of the peak of the fresh PSi layer. This is in accordance with the reported PL drop in some cases [16–18]. Even after oxidation at higher temperature, the PL is observed and found to be stabilised in our study as reported by Petrova-Koch et al. [19].

In order to assess the PSi based optoelectronic devices for various applications, the device should have high efficiency and good stability over a long period of time under oxidizing atmospheric conditions. In this aspect the junction was formed by heating at 400 °C. The effect of heating and aging on the PL properties was studied.

Fig. 6a and b shows the PL spectra of as prepared SnO$_2$/PSi and heated junctions. The PL profile of thin SnO$_2$ film coated on PSi shows a peak at 633 nm and a small hump at about 700 nm. This symmetry may be due to the incorporation of SnO$_2$ into the
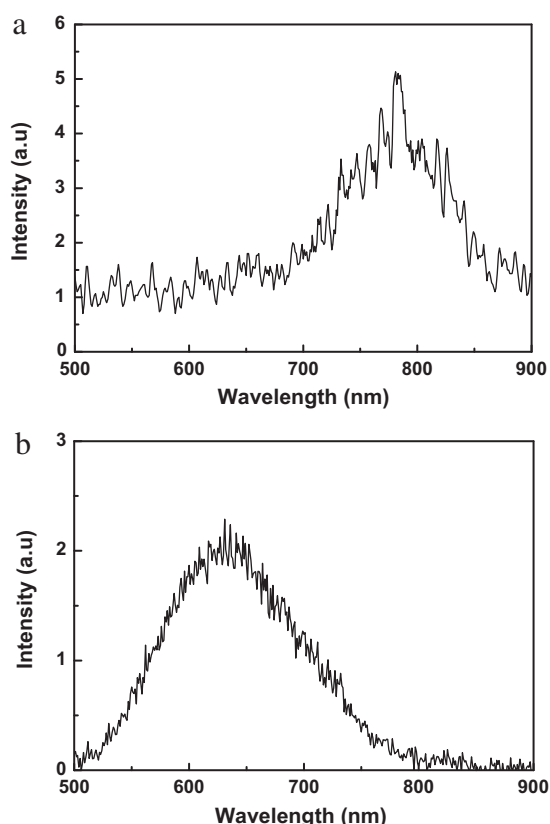
Fig. 6. Photoluminescence spectra of SnO_2/PSi junction (a) as-prepared and (b) aged for two months.

pores and the shift to higher wavelength may be due to the slightly enlarged shape and size of PSi coated over the silicon pillars with SnO_2. This is also confirmed by the XRD results, where XRD peaks pertaining to SnO_2 and PSi are observed showing a preferred orientation along (1 1 0) direction. Fig. 6b shows the PL spectra of SnO_2/PSi structure aged for two months. Though the intensity is reduced, it is found to be stabilised which is an advantage for developing solar cells using this structure. Further, the shift of peak to about 633–650 nm suggests that SnO_2 not only modifies the nature of nanopores but also is expected to influence the interface states in SnO_2/PSi junction. Similar results for aluminium sputtering [20] and Si–Fe bonds on the PSi surface are observed where the aging effect is reduced and the structures are stabilised.

It is well known that luminescence properties of PSi are very sensitive to the surface structure. Kanemitsu et al. [21] showed that a strong red and blue PL was observed from oxidized PSi by the rapid thermal oxidation process. The red PL emission observed was due to a radiative recombination of excitons in the surface region in the Si crystallite and the blue PL originated from a recombination of excitons confined in crystalline Si (c-Si) core [21]. It was further stated that two types of Si:O compounds on the surface structure of the c-Si core took place. One is when the surface of c-Si core is covered by silicon oxyhydrides (Si:O:H) and silicon oxides (Si:O) where oxygen atoms cannot migrate into the Si network at low oxidation temperature ($T < 800\,°C$). The other is when the surface of the c-Si core is covered by an amorphous SiO_2 (a-SiO_2) layer where oxygen atoms migrate into the Si-skeleton layer and oxygen atoms form the bridge. Although the a-SiO_2 layer does not itself contribute to visible PL; it can create an electronic state in an interfacial region between the c-Si core and the a-SiO_2 layer. The SnO_2 deposition onto the PSi surface may similarly have led to the formation of an interfacial region where photogenerated electrons, holes and excitons are confined. The deposition onto PSi surface may also play the role of SiO_2 as an energetic barrier preventing the escape of the photogenerated carriers outside the confined crystallites. This observation is similar to that observed in ZnO coated PSi [22].

4. Conclusions

Steps to produce PSi layer with desired properties are optimized. PSi formed at $30\,mA/cm^2$ shows that it can be used effectively in the development of light emitting diodes. The XRD and PL studies confirm the presence of silicon nanocrystallites and networks in the PSi structure. SnO_2/PSi junctions formed using the above conditions show good stability under aging.

References

[1] C.D. Feng, Y. Shimizu, M. Egashira, J. Electrochem. Soc. 141 (1994) 220–225.
[2] Y. Takahashi, Y. Wada, J. Electrochem. Soc. 137 (1990) 267–272.
[3] S.S. Park, H. Zheng, J.D. Mackenzie, Mater. Lett. 22 (1995) 175–180.
[4] C.J. Brinker, G.W. Scherer, Sol–Gel Science, The Physics and Chemistry of Sol–Gel Processing, Academic Press, San Diego, 1990.
[5] H. Elhouichet, A. Moadhen, M. Oueslati, S. Romdhane, J.A. Roger, H. Bouchriha, Physica Status Solidi C 2 (2005) 3349.
[6] D. Bellet, G. Dolino, Thin Solid Films 276 (1996) 1.
[7] D. Buttard, D. Bellet, G. Dolino, T. Baumbach, J. Appl. Phys. 83 (1998) 5814.
[8] L. Abello, B. Bochu, A. Gaskov, S. Koudryatseva, G. Lucazeau, M. Roumyantseva, J. Solid State Chem. 135 (1998) 78.
[9] Z.W. Chen, J.K.I. Lai, C.H. Shek, H.D. Chen, Appl. Phys. A 81 (2005) 1073.
[10] P.M. Fauchet, J. Lumin. 80 (1999) 53.
[11] R.S. Dubey, D.S. Gautam, Opt. Quantum Electron. 41 (2009) 189.
[12] H.S. Mavi, B.G. Rasheed, R.K. Soni, S.C. Abbi, K.P. Jain, Thin Solid Films 397 (2001) 125.
[13] D.J. Lockwood, A. Wang, Solid State Commun. 94 (1995) 905.
[14] A.G. Cullis, L.T. Canham, O.D. Dosser, Res. Soc. Symp. Proc. Mater. 256 (1992) 7.
[15] I. Berbezier, A. Halimaoui, J. Appl. Phys. 74 (1993) 5421.
[16] L.T. Canham, M.R. Houlton, W.Y. Leong, C. Pickering, J.M. Keen, J. Appl. Phys. 70 (1991) 422.
[17] T. Maruyama, S. Ohtani, Appl. Phys. Lett. 65 (1994) 1346.
[18] S. Shih, C. Tsai, K.H. Li, K.H. Jung, J.C. Campbell, D.L. Kwong, Appl. Phys. Lett. 60 (1992) 633.
[19] V. Petrova-Koch, T. Muschik, A. Kux, B.K. Meyer, F. Koch, V. Lehmann, Appl. Phys. Lett. 61 (1992) 943.
[20] Y.H. Zhang, X.J. Li, L. Zheng, Q.W. Chen, Phys. Rev. Lett. 81 (1998) 1710.
[21] Y. Kanemitsu, T. Futagi, T. Matsumoto, H. Mimura, Phys. Rev. B 49 (1994) 14732.
[22] .E. Kahayan, J. Lumin. 130 (2010) 1295.